

Leggett-Garg Inequalities for Squeezed States

Jérôme Martin^{1,*} and Vincent Vennin^{2,†}

¹*Institut d'Astrophysique de Paris, UMR 7095-CNRS,
Université Pierre et Marie Curie, 98 bis boulevard Arago, 75014 Paris, France*

²*Institute of Cosmology and Gravitation, University of Portsmouth,
Dennis Sciama Building, Burnaby Road, Portsmouth, PO1 3FX, United Kingdom*

(Dated: February 15, 2022)

Temporal Bell inequalities, or Leggett-Garg Inequalities (LGI), are studied for continuous-variable systems placed in a squeezed state. The importance of those systems lies in their broad applicability, which allows the description of many different physical settings in various branches of physics, ranging from cosmology to condensed matter physics and from optics to quantum information theory. LGI violations are explored and systematically mapped in squeezing parameter space. Configurations for which LGI violation occurs are found, but it is shown that no violation can be obtained if all squeezing angles vanish, contrary to what happens for the spatial Bell inequalities. We also assess the effect of decoherence on the detectability of such violations. Our study opens up the possibility of new experimental designs for the observation of LGI violation.

PACS numbers: 03.65.-w, 03.67.-a, 03.65.Ud, 03.67.Mn, 03.65.Ta

I. INTRODUCTION

One of the most interesting aspects of quantum mechanics is the possibility of having entangled states [1]. Surprising properties of these states are revealed by Bell's inequalities [2, 3], which highlight the non-classical correlations that can exist between spatially-separated subsystems [4, 5]. However, quantum mechanics may also imply the presence of non-standard correlations when a single system is measured at two different times. These correlations can be studied by deriving another class of inequalities, known as temporal Bell inequalities or Leggett-Garg inequalities (LGI) [6]. A violation of these inequalities can be caused by the lack of a realistic description of the system (macroscopic realism) or by the impossibility to measure its properties without disturbing it (non-invasive measurability). Therefore, LGI violations have deep and far-reaching implications for quantum mechanics and physics in general [7].

On the experimental side, violations of LGI have now been observed in different systems, for a review see Ref. [7]. These systems all share the property of being effectively describable as a qubit. Originally, it was proposed to use a rf SQUID to perform the test [6]. The rf SQUID is a magnetic flux box made of a Josephson junction inserted into a superconducting ring and controlled by an external flux. If the external flux is tuned to half the quantum flux, then the potential of the system acquires a double-well shape, the lowest energy states in each well effectively decouple, and the rf SQUID can be viewed as a qubit. The two states correspond to clockwise and anticlockwise super-current states. In practice, the first LGI violation was in fact observed in a transmon [8],

a device similar to a Cooper-pair box (a Josephson junction driven by an applied voltage) but operated in a different regime [9]. In that case, the qubit is represented by the $|0\rangle$ and $|1\rangle$ charge states. Since this experiment, many other protocols have been considered, in particular the recent proposals studied in Refs. [10, 11]. Let us note that LGI violations have also been observed for other systems [7] equivalent to a qubit but not necessarily based on superconducting circuits.

The non-invasive measurability principle, which has been the subject of many debates, has also played an important role in the design of the different experimental systems. In the original proposal [6], the measurements were assumed to be performed in the usual, projective, fashion. However, in the first experimental realization of Ref. [8], continuous weak measurements were used, following Ref. [12], which required one to adapt the original form of the LGI to the situation at hand. The subsequent experimental setups then considered various variations of the measurement protocol.

In this paper we propose and study a new and generic way to design physical situations in which the LGI are violated. Concretely, our approach applies to any continuous-variable system placed in a quantum squeezed state [13, 14]. These states are entangled states and arise in a large variety of physical situations. The reason is that any Hamiltonian that is bilinear in the creation and annihilation operators is likely to produce squeezed states. One finds them in experiments with light fields using lasers and non-linear optics (parametric down-conversion, four-wave mixing) [15, 16] or experiments probing the motion of an ion in a trap or the properties of phonons in a crystal [17]. Squeezed states are also unavoidable when a quantum field interacts with a classical source as is the case in the Schwinger [18], Unruh [19] and Hawking [20] effects. Moreover, according to the theory of cosmic inflation [21–23], recently confirmed by the Planck satellite data [24–29], the quan-

*Electronic address: jmartin@iap.fr

†Electronic address: vincent.vennin@port.ac.uk

tum state of the cosmological fluctuations responsible for the Cosmic Microwave Background Radiation (CMBR) anisotropy and the large scale structures observed in our universe, is a (two-mode) squeezed state [30–33]. Let us add that squeezed states are also very useful for interferometric measurements (which, for instance, are used for the detection of gravitational waves [34]) or to improve the precision of atomic clocks [35]. They also play a crucial role in quantum information processing [36]. Finally, it is interesting to note that entangled states were introduced for the first time in their squeezed state realization since the Einstein-Podolski-Rosen (EPR) state [1] is nothing but a squeezed state with infinite squeezing.

Let us also stress that a fundamental difference with qubits is that squeezed states describe continuous variable systems (see also Ref. [37]). Besides opening up possibilities of new experimental LGI violations, this may also provide a way to test the quantumness of primordial cosmological fluctuations [33], the possibility of which is still being debated.

This paper is organized as follows. In Sec. II, we introduce spin operators for continuous-variable systems and calculate their two-point correlation functions. In Sec. III, we then show that LGI can be violated and we map the LGI violations in the space of the squeezing parameters and squeezing angles. Finally, we present our conclusions in Sec. IV. The appendix A contains technical details needed to derive the results discussed in the main text.

II. SPIN OPERATORS FOR SQUEEZED STATES

We consider a quantum system that possesses continuous degrees of freedom denoted in the following by Q ; Q could, for instance, be the position of a particle or the Fourier amplitude of a field at a given wave number. In order to test the LGI, one needs to define a dichotomic quantity and, for this reason, we introduce the following operator

$$\hat{S}_z(\ell) = \sum_{n=-\infty}^{n=+\infty} (-1)^n \int_{n\ell}^{(n+1)\ell} dQ |Q\rangle \langle Q|, \quad (1)$$

where ℓ is a parameter that can be freely chosen by the observer and that describes the coarseness of the measurement (the larger ℓ , the coarser the measurement). In the limit where $\ell \rightarrow \infty$, for instance, $\hat{S}_z(\ell)$ is simply the sign of Q . In general, Eq. (1) defines a spin variable because the eigenvalues of this operator are ± 1 (for an alternative way of defining dichotomic variables see Ref. [38]). It is similar to the z -component of a fictitious spin. As explained in Ref. [39], one could define two other operators, $\hat{S}_x(\ell)$ and $\hat{S}_y(\ell)$ such that $\hat{S}_x(\ell)$, $\hat{S}_y(\ell)$ and $\hat{S}_z(\ell)$ obey the standard $SU(2)$ commutation relations. Here, we will only need $\hat{S}_z(\ell)$. It is not the only way to define a “spin” from a continuous-variable

system and we could also consider the operator [40, 41] $\sum_{n=0}^{+\infty} (|2n+1\rangle\langle 2n+1| - |2n\rangle\langle 2n|) = (-1)^{\hat{N}+1}$ where $|n\rangle$ are the Fock states and \hat{N} is the number operator. However, in this case, it is not obvious how to design an experimental protocol to perform a measurement of $(-1)^{\hat{N}+1}$ while measuring the quantity (1) is straightforward since only “position” measurements are needed. In this sense, the choice (1) of $\hat{S}_z(\ell)$ appears to be essentially unique. Note that Bell inequalities formed out of the triplet $\hat{S}_x(\ell)$, $\hat{S}_y(\ell)$ and $\hat{S}_z(\ell)$ can be violated if the system is placed in a squeezed state as recently shown in Refs. [39, 42]. However, this involves the measurements of, at least, two spin operators and measuring $\hat{S}_x(\ell)$ and/or $\hat{S}_y(\ell)$ requires the measurement of the conjugate momentum of \hat{Q} , which may be difficult (e.g. in inflationary cosmology, this appears to be essentially impossible [33]). The advantage of the LGI is that only one operator is necessary, the price to pay being of course that one has to measure it at three different times.

Then, we assume that the system is placed in the quantum state $\hat{U}|0\rangle$, a (one-mode) squeezed state, where the evolution operator \hat{U} can be written as $\hat{U}(t) = e^{\hat{B}(t)}$ with $\hat{B}(t) \equiv r(t)e^{-2i\varphi(t)}\hat{a}^2/2 - r(t)e^{2i\varphi(t)}(\hat{a}^\dagger)^2/2$, where \hat{a} and \hat{a}^\dagger are, respectively, the annihilation and creation operators satisfying $[\hat{a}, \hat{a}^\dagger] = 1$. The quantities $r(t)$ and $\varphi(t)$ are respectively the squeezing parameter and angle and are typically time-dependent quantities.

In the following, we will be interested in the calculation of the two-point correlation function of the spin operator (1) taken at different times, namely

$$C_{ab}(t_a, t_b; \ell) = \frac{1}{2} \langle 0 | \left\{ \hat{S}_z(t_a; \ell), \hat{S}_z(t_b; \ell) \right\} | 0 \rangle, \quad (2)$$

where $\hat{S}_z(t, \ell)$ is written in the Heisenberg picture, namely $\hat{S}_z(t, \ell) \equiv U^\dagger(t) \hat{S}_z(\ell) \hat{U}(t)$. This gives rise to (see the appendix for the following formulas)

$$C_{ab} = \Re \left[\mathcal{A}(a, b) \sum_{n=-\infty}^{n=+\infty} \sum_{m=-\infty}^{m=+\infty} (-1)^{n+m} \int_{n\ell}^{(n+1)\ell} \int_{m\ell}^{(m+1)\ell} d\tilde{Q} d\bar{Q} e^{A(a,b)\tilde{Q}^2 + A^*(b,a)\bar{Q}^2 + B(a,b)\tilde{Q}\bar{Q}} \right] \quad (3)$$

with (see the *erratum* section at the very end)

$$\begin{aligned} \mathcal{A}(a, b) &= \frac{1}{\pi\sqrt{2}} \frac{\sin^{-1/2}(\theta_a - \theta_b)}{\rho_a \rho_b \cosh r_a \cosh r_b} e^{i(\theta_a - \theta_b - \pi/2)/2}, \quad (4) \\ \mathcal{A}(a, b) &= \frac{1}{2} - \frac{\cos \theta_a}{\rho_a} + \frac{i \cos \theta_b}{\rho_a \sin(\theta_a - \theta_b)} \\ &\quad - i \frac{\sin \theta_a}{\rho_a} - \frac{i}{2 \tan(\theta_a - \theta_b)}, \quad (5) \\ \mathcal{B}(a, b) &= -\frac{i}{\rho_a \rho_b \sin(\theta_a - \theta_b)} \frac{1}{\cosh r_a \cosh r_b}, \quad (6) \end{aligned}$$

where ρ and θ are defined so that $1 - \tanh(r)e^{2i\varphi} \equiv \rho e^{i\theta}$. In general, these integrations must be performed numeri-

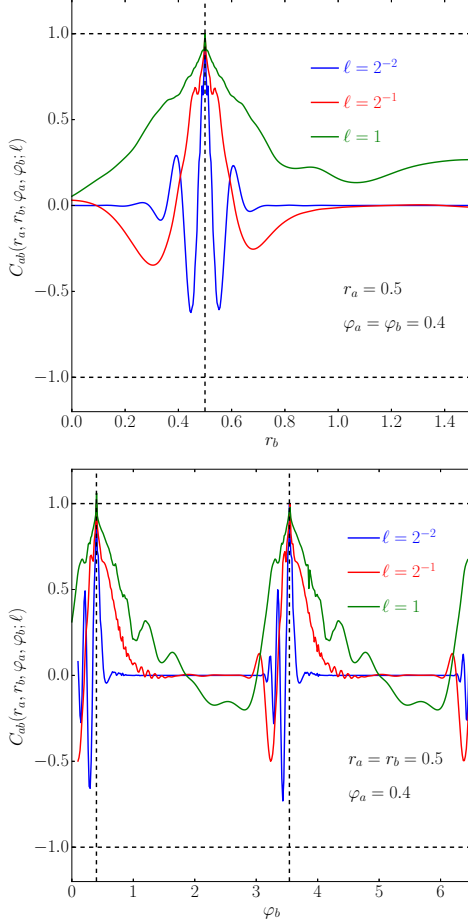


FIG. 1: Two-point function of the spin operator, the system being placed in a squeezed state with squeezing parameter and angle (r_a, φ_a) at time t_a and (r_b, φ_b) at time t_b , as a function of r_b (top panel) and φ_b (bottom panel), for a few values of ℓ .

cally.¹ However, if we are considering the case where the squeezing angles all vanish, then the integrations can be done and the series reduces to $C_{ab} = \sum_{n=-\infty}^{n=+\infty} (-1)^n C_n$ with

$$C_n = \frac{1}{2} (-1)^{E(r_a - r_b n)} \{ 2 \operatorname{erf} [e^{r_b} E(e^{r_a - r_b n}) \ell + e^{r_b} \ell] - \operatorname{erf} [e^{r_a} (n+1) \ell] - \operatorname{erf} (e^{r_a} n \ell) \}, \quad (7)$$

if the condition $e^{r_b - r_a} [E(e^{r_a - r_b n}) + 1] < n+1$ is satisfied, while

$$C_n = \frac{1}{2} (-1)^{E(r_a - r_b n)} \{ \operatorname{erf} [e^{r_a} (n+1) \ell] - \operatorname{erf} (e^{r_a} n \ell) \} \quad (8)$$

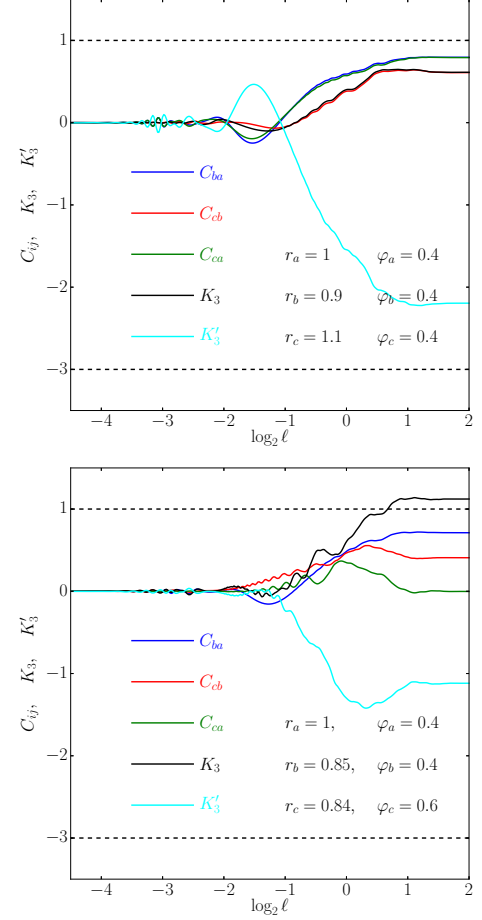


FIG. 2: Two-point function (2) of the spin operator (1) and Leggett-Garg strings (10) for the squeezed state measured at times t_a , t_b and t_c , as a function of ℓ . LGI violations correspond to K_3 or K'_3 being either smaller than -3 or greater than 1 . For the parameters used in the bottom panel for instance, violation $K_3 > 1$ occurs at large ℓ .

otherwise. In these expressions, erf is the error function and $E(z)$ denotes the integer part of the number z . Another case where a simple analytic expression can be derived is the limit $\ell \rightarrow \infty$, where one obtains [see Eq. (A20) in Appendix A]

$$C_{ab} = \Re \left\{ -\frac{4A \operatorname{arctanh} [B/\sqrt{B^2 - 4AA^*}]}{\sqrt{B^2 - 4AA^*}} \right\} \quad (9)$$

that is to say a plateau, independent of ℓ .

¹ A FORTRAN code for computing the two-point correlation function of the spin operators, the 3-measurement Leggett-Garg strings and all quantities displayed in this paper can be found at <https://github.com/vennin/LeggettGargInequalities>.

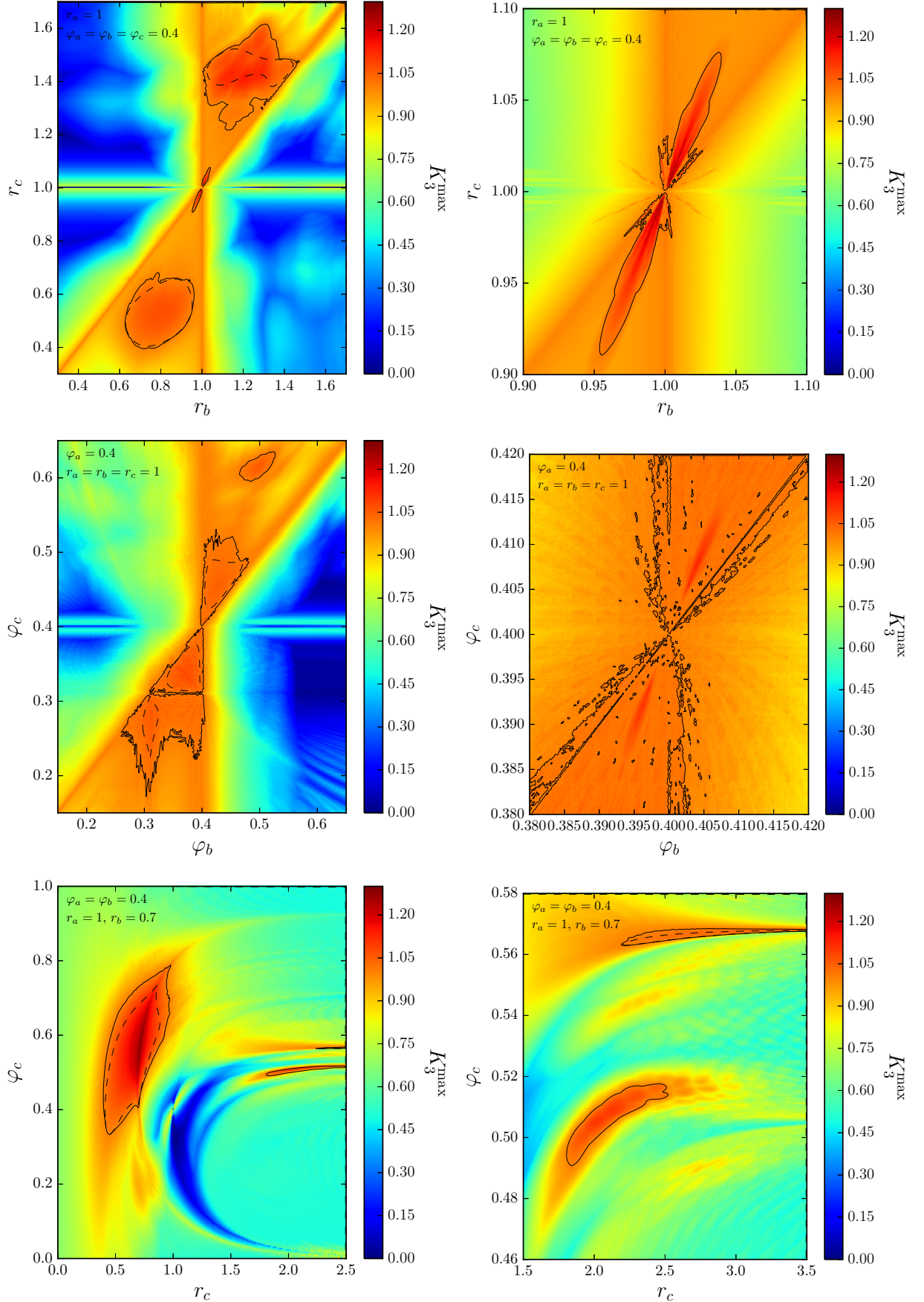


FIG. 3: Maximal values over ℓ of the Leggett-Garg strings K_3 as a function of the squeezing parameters. The black solid lines correspond to the contours where the strings equal one and inside which LGI violation occurs. The dashed lines stand for the same contours but where ℓ is taken to infinity instead of maximized over. The right panels zoom in on regions of interest of the left panels. The top panels show $r_a = 1$ and $\varphi_a = \varphi_b = \varphi_c = 0.4$, the middle panels $\varphi_a = 0.4$ and $r_a = r_b = r_c = 1$, and the bottom panels $\varphi_a = \varphi_b = 0.4$, $r_a = 1$, and $r_b = 0.7$.

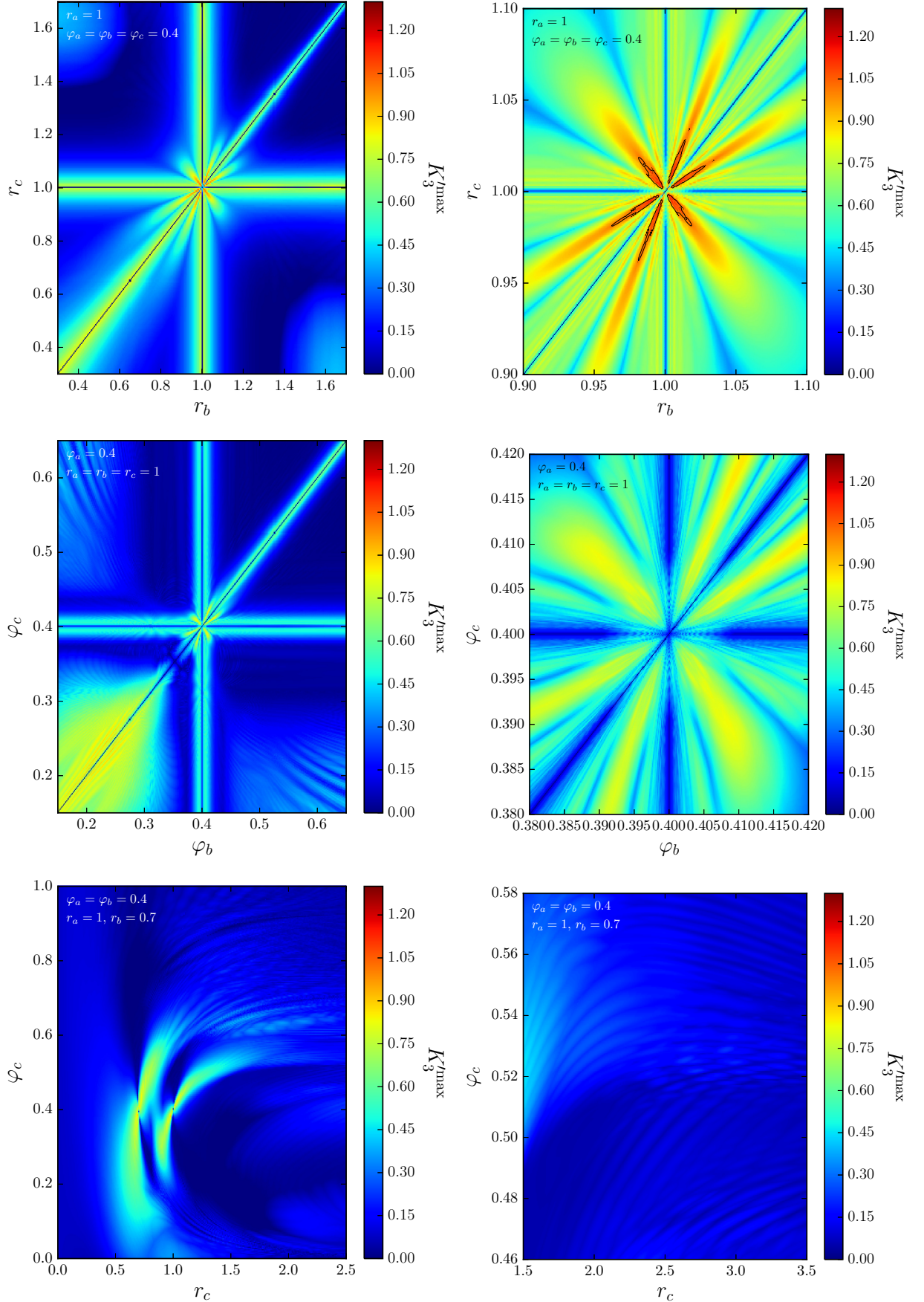


FIG. 4: Maximal values over ℓ of the Leggett-Garg strings K'_3 as a function of the squeezing parameters. The black solid lines correspond to the contours where the strings equal one and inside which LGI violation occurs. The dashed lines stand for the same contours but where ℓ is taken to infinity instead of maximized over. The right panels zoom in on regions of interest of the left panels. The top panels show $r_a = 1$ and $\varphi_a = \varphi_b = \varphi_c = 0.4$, the middle panels $\varphi_a = 0.4$ and $r_a = r_b = r_c = 1$, and the bottom panels $\varphi_a = \varphi_b = 0.4$, $r_a = 1$, $r_b = 0.7$.

In Fig. 1, we have represented the evolution of the correlation function versus the squeezing parameter r and the squeezing angle φ for different choices of ℓ . When $r_a = r_b$ and $\varphi_a = \varphi_b$, the correlation function is of course one. Otherwise one can check that it is always between ± 1 and that it tends to zero when $|r_b - r_a|$ or $|\varphi_a - \varphi_b|$ becomes sufficiently large.

III. LEGGETT-GARG INEQUALITIES

Let us now introduce the so-called 3-measurement Leggett-Garg strings K_3 and K'_3 (which, if needed, could easily be generalized to n -strings) defined by

$$K_3 = C_{ab} + C_{bc} - C_{ac}, \quad K'_3 = -C_{ab} - C_{bc} - C_{ac}, \quad (10)$$

where a , b and c denote the three times (in chronological order) when the measurement is performed. Classical probability calculus implies $-3 \leq K_3, K'_3 \leq 1$ and, therefore, any deviation from those inequalities will be referred to as a LGI violation. If the state of the system is a qubit $\hat{\sigma}_z$ with density matrix $\rho = [1 + \mathbf{r}(t) \cdot \boldsymbol{\sigma}]/2$ (\mathbf{r} is the unit Bloch vector and $\boldsymbol{\sigma}$ are the Pauli matrices) and Hamiltonian $\hat{H} = \omega \hat{\sigma}_x/2$ (ω is the fundamental frequency of the system), then the correlation function of $\hat{\sigma}_z$ is simply given by $C_{ij} = \cos[\omega(t_i - t_j)]$. Choosing equal time intervals $t_c - t_b = t_b - t_a \equiv \tau$, one obtains $K_3 = 2 \cos(\omega\tau) - \cos(2\omega\tau)$ which clearly violates the LGI, the maximum violation being obtained for $\omega\tau = \pi/3$ for which $K_3 = 3/2$. An important remark is that the correlators C_{ij} , hence the strings K_3 and K'_3 , do not depend on the state $\mathbf{r}(t)$ of the qubit. As can be seen in Fig. 1, this is not the case for the squeezed state where there is a dependence on the parameters characterizing the quantum state.

The 3-strings K_3 and K'_3 are displayed in Fig. 2 as a function of ℓ for different configurations. One can see that in some cases (top panel), LGI are not violated, while for others (bottom panel), there exist values of ℓ for which they are. In practice, making use of the formulas (7) and (8) for C_n , one can check that when all squeezing angles vanish, no violation can be obtained. This is in contrast to Bell inequalities constructed from the same spin operators [42], where violation requires $\varphi < 0.34e^{-r}$ and is maximal precisely for vanishing squeezing angles. Another important difference between these two inequalities is that while Bell inequalities violation requires $r > 1.12$ [42], LGI violation occurs even for small squeezing parameters.

In order to further explore LGI violation in squeezing parameter space, in Figs. 3 and 4, the maximal values of K_3 and K'_3 are displayed as a function of the squeezing parameters, where maximization is performed over ℓ . We did not find configurations for which the classical conditions $K_3, K'_3 \geq -3$ are violated which is why only the maximal values of K_3 and K'_3 are shown. The right panels zoom in on interesting features of the left panels. The black solid lines correspond to the contours $K_3, K'_3 = 1$,

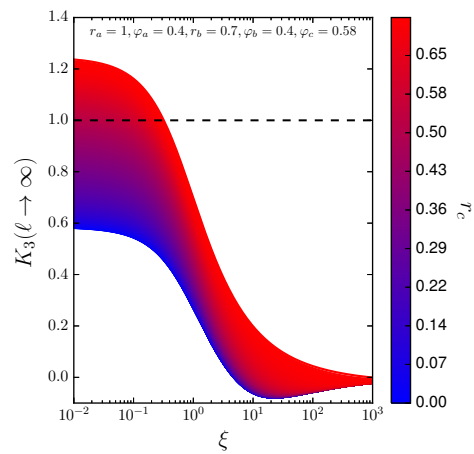


FIG. 5: Leggett-Garg 3-string K_3 as a function of the decoherence parameter ξ , in the limit $\ell \rightarrow \infty$ and for a set of squeezing parameters, where r_c is varied according to the color code. When ξ is of order one or larger, no violation occurs.

and violation occurs inside them. The overall structure of these maps is rather complex and usually features several disconnected regions of parameter space where violation occurs. Such regions typically correspond to where the different squeezing parameters are close but not strictly equal (see the top right and middle right panels of Fig. 3 and the top right panel of Fig. 4) but can also exist away from these conditions (left panels and bottom right panel in Fig. 3). Notice that the non-smooth shapes of the contours are not numerical artifacts but correspond to genuine irregular patterns. The dashed lines stand for the contours $K_3, K'_3 = 1$ but when ℓ is taken to infinity instead of maximized over. In this case, K_3 and K'_3 can easily be calculated using Eq. (9), and as mentioned above, the measurement of \hat{S}_z is simply performed by measuring the sign of the position variable. This regime is therefore experimentally convenient. However, one can see that in some regions (i.e. inside the solid contours but outside the dashed contours), violation does not occur on the asymptotic plateau $\ell \rightarrow \infty$ but can be obtained for a bounded interval of ℓ values only. Even though this interval may be fine-tuned, ℓ can be freely chosen by the experimenter so this does not hamper the practical detection of LGI violation.

More generally, Figs. 3 and 4 can be used to identify the values of r and φ where LGI violations occur. Given a particular experimental setting, corresponding to a particular range for r and φ , one can indeed immediately check whether a LGI violation is possible or not. As a consequence, these maps hopefully constitute a useful guide for designing new experimental protocols.

IV. CONCLUSIONS

In this paper, we have shown how LGI violation can be obtained with continuous-variable systems, and have illustrated our approach on the generic case of squeezed states. By doing so, we have widely extended the range of systems for which LGI violation can be realized, so far limited to qubits.

In practice, measuring the spin operator (1) from a measurement of the “position” variable Q is straightforward; one simply needs to determine which integer number n is such that $n\ell \leq Q < (n+1)\ell$, and take $S_z = (-1)^n$. This is why ℓ can be easily varied over until the largest violation is found and this parameter can be optimized as done in Figs. 3 and 4. Let us note that if one also has access to linear combinations of Q and its conjugated momentum P , there is an overall shift in the squeezing angles that one can also optimize over. Indeed, if one performs a rotation in phase space with angle α and introduces $Q' = \cos \alpha Q - \sin \alpha P$ and $P' = \cos \alpha P + \sin \alpha Q$, then the squeezing angles change according to $\varphi' = \varphi + \alpha$ [42]. As a consequence, if one defines the pseudo-spin operators with respect to Q' instead of Q , one obtains the same results as the ones derived above but where all the squeezing angles are shifted by α .

Since LGI probe correlations of a single system measured at different times, quantum decoherence [43–45] also plays a crucial role for a realistic and practical experiment [8, 46]. The effect of decoherence can be modeled using the quantum channels formalism [47]. For a qubit system, only a few channels exist and they can be studied separately [48, 49]. For a continuous-variable system, however, the dimension of the Hilbert space is infinite and such a systematic approach cannot be employed without specifying the environment. In order to assess the impact of decoherence on our results in a more model-independent way, one can consider the simple channel in which the density matrix ρ is mapped onto [45] $\rho(\tilde{Q}, \tilde{Q}) \rightarrow \rho(\tilde{Q}, \tilde{Q}) \exp[-\xi(\tilde{Q} - \bar{Q})^2/2]$, where the phenomenological parameter ξ encodes the details of the interaction strength with the environment. In Eq. (3), this amounts to changing A and B according to $A \rightarrow A - \xi/2$ and $B \rightarrow B - \xi$. This models the situation where dynamical backreaction is small and decoherence is slower than the unitary evolution of the state. In Fig. 5, the 3-string K_3 is displayed for a set of squeezing parameters (where r_c is varied according to the color code) as a function of ξ and in the limit where $\ell \rightarrow \infty$.

When ξ increases, coherence is lost and K_3 is driven to 0. In the case where LGI are violated at $\xi = 0$, one can see that no violation occurs when ξ is of order one or larger. This is why limiting the coupling with the environment is important for a practical implementation of the proposal made in this paper.

Erratum

After this article was published, we noticed that Eq. (5), in which $A(a, b)$ is defined, contained a typo, which has been corrected in the present version. Since all other formulas do not depend on the precise definition of $A(a, b)$, the rest of the calculation is not affected. However, the figures would need to be redone, since they were derived using the previous version of Eq. (5). We have nonetheless checked that this does not alter our main conclusion, namely that one can still find configurations where the Leggett-Garg inequalities are violated. For instance, for $r_a = 0.49$, $r_b = 0.77$, $r_c = 1.12$, $\varphi_a = 0.26$, $\varphi_b = 0.27$ and $\varphi_c = 0.4$, the corrected formula gives $K_3 \simeq 1.101$ for $\ell = 3$.

Moreover, we have realised that, following common practice, we discarded an overall phase in the wavefunction. While measurements performed at the same time are insensitive to such an overall phase, this is not the case for multiple-time measurements for which the result is sensitive to the change in the overall phase between the measurement times. See Ref. [50] for further details and for a calculation that includes this possible phase change. Our result therefore applies only to the case where the overall phase does not vary in time. Yet, this again does not alter our main conclusion, namely that one can find configurations where the Leggett-Garg inequalities are violated by two-mode squeezed states.

Acknowledgments

V.V. acknowledges financial support from STFC grants ST/K00090X/1 and ST/N000668/1. Numerical computations were done on the Sciama High Performance Compute cluster which is supported by the ICG, SEPNet and the University of Portsmouth. We thank Kenta Ando for pointing out a typo in Eq. (5).

Appendix A: Calculation of the two-point correlation function

In this appendix, we explain how the two-point correlation function is calculated. Using the expression of the correlator (2) and the definition of the spin operator (1), one obtains

$$C_{ab} = \sum_{n=-\infty}^{n=+\infty} \sum_{m=-\infty}^{m=+\infty} (-1)^{n+m} \int_{n\ell}^{(n+1)\ell} \int_{m\ell}^{(m+1)\ell} d\tilde{Q} d\bar{Q} \Re \left[\Psi_{1sq}^*(t_a, \tilde{Q}) \Psi_{1sq}(t_b, \bar{Q}) \langle \tilde{Q} | \hat{U}(t_a) \hat{U}^\dagger(t_b) | \bar{Q} \rangle \right], \quad (A1)$$

where $\Psi_{1\text{sq}}$ denotes the (single-mode) squeezed state wave function given by the following expression

$$\Psi_{1\text{sq}}(t, Q) = \frac{1}{\pi^{1/4}} \frac{1}{\sqrt{\cosh r}} \frac{1}{\sqrt{1-z}} e^{-(1+z)/(1-z)Q^2/2}, \quad (\text{A2})$$

with $z \equiv e^{2i\varphi} \tanh r$. Notice that this wave function is correctly normalized. Inserting three times the closure relation for coherent states, the matrix element appearing in Eq. (A1) can be re-expressed as

$$\langle \tilde{Q} | \hat{U}(t_a) \hat{U}^\dagger(t_b) | \bar{Q} \rangle = \int \frac{du}{\pi} \int \frac{dv}{\pi} \int \frac{dw}{\pi} \langle \tilde{Q} | w \rangle \langle w | \hat{U}(t_a) | u \rangle \langle u | \hat{U}^\dagger(t_b) | v \rangle \langle v | \bar{Q} \rangle. \quad (\text{A3})$$

Matrix elements of the form $\langle w | \hat{U}(t) | u \rangle$ can be easily calculated using the operator ordering theorem applied to the evolution operator \hat{U} and quantities such as $\langle v | \bar{Q} \rangle$ are nothing but the coherent states wave function in the configuration representation. As a consequence, one arrives at the following expression

$$\langle \tilde{Q} | \hat{U}(t_a) \hat{U}^\dagger(t_b) | \bar{Q} \rangle = \frac{1}{\pi^{7/2}} \frac{1}{\sqrt{\cosh r_a \cosh r_b}} e^{-\tilde{Q}^2/2 - \bar{Q}^2/2} \int d^6\alpha e^{-\alpha^T M \alpha/2 - J^T \alpha}, \quad (\text{A4})$$

with $\alpha^T \equiv [\Re(u), \Im(u), \Re(v), \Im(v), \Re(w), \Im(w)]$ and $J^T = -\sqrt{2}(0, 0, \bar{Q}, -i\bar{Q}, \tilde{Q}, i\tilde{Q})$. The quantity M is a 6×6 symmetric matrix whose elements can be written as

$$M_{11} = 2 - e^{-2i\varphi_a} \tanh r_a - e^{2i\varphi_b} \tanh r_b, \quad M_{12} = -ie^{-2i\varphi_a} \tanh r_a + ie^{2i\varphi_b} \tanh r_b, \quad (\text{A5})$$

$$M_{13} = -\frac{1}{\cosh r_b}, \quad M_{14} = -\frac{i}{\cosh r_b}, \quad M_{15} = -\frac{1}{\cosh r_a}, \quad M_{16} = \frac{i}{\cosh r_a}, \quad (\text{A6})$$

$$M_{22} = 2 + e^{-2i\varphi_a} \tanh r_a + e^{2i\varphi_b} \tanh r_b, \quad M_{23} = \frac{i}{\cosh r_b}, \quad M_{24} = -\frac{1}{\cosh r_b}, \quad (\text{A7})$$

$$M_{25} = -\frac{i}{\cosh r_a}, \quad M_{26} = -\frac{1}{\cosh r_a}, \quad M_{33} = 3 + e^{-2i\varphi_b} \tanh r_b, \quad (\text{A8})$$

$$M_{34} = -i + ie^{-2i\varphi_b} \tanh r_b, \quad M_{35} = M_{36} = 0, \quad M_{44} = 1 - e^{-2i\varphi_b} \tanh r_b, \quad M_{45} = M_{46} = 0 \quad (\text{A9})$$

$$M_{55} = 3 + e^{2i\varphi_a} \tanh r_a, \quad M_{56} = i - ie^{2i\varphi_a} \tanh r_a, \quad M_{66} = 1 - e^{2i\varphi_a} \tanh r_a. \quad (\text{A10})$$

From these formula it is straightforward to calculate the determinant of the matrix M . It reads

$$\det M = -128i [\sin(2\varphi_a) \tanh r_a - \sin(2\varphi_b) \tanh r_b - \sin(2\varphi_a - 2\varphi_b) \tanh r_a \tanh r_b]. \quad (\text{A11})$$

This determinant vanishes when the two times at which the correlation function is calculated are the same. Moreover, if $\varphi_a = \varphi_b = 0$ (but, possibly, $r_a \neq r_b$), the determinant is also zero. These two cases must be treated separately.

Let us first assume that $\det M \neq 0$. Then, the Gaussian integral (A4) can easily be performed and one finds

$$\langle \tilde{Q} | \hat{U}(t_a) \hat{U}^\dagger(t_b) | \bar{Q} \rangle = \frac{8}{\sqrt{\pi}} \frac{1}{\sqrt{\cosh r_a \cosh r_b}} e^{-\tilde{Q}^2/2 - \bar{Q}^2/2} \frac{1}{\sqrt{\det M}} e^{J^T M^{-1} J/2}. \quad (\text{A12})$$

Clearly, this matrix element is a Gaussian function in \tilde{Q} and \bar{Q} since $J^T M^{-1} J$ is a quadratic form in \tilde{Q} and \bar{Q} , explicitly

$$\begin{aligned} \frac{1}{2} J^T M^{-1} J = & -\frac{64}{\det M} (1 - e^{-2i\varphi_a} \tanh r_a + e^{-2i\varphi_b} \tanh r_b - e^{2i\varphi_a - 2i\varphi_b} \tanh r_a \tanh r_b) \bar{Q}^2 \\ & - \frac{64}{\det M} (1 + e^{2i\varphi_a} \tanh r_a - e^{2i\varphi_b} \tanh r_b - e^{2i\varphi_a - 2i\varphi_b} \tanh r_a \tanh r_b) \tilde{Q}^2 + \frac{128}{\det M} \frac{\bar{Q} \tilde{Q}}{\cosh r_a \cosh r_b}. \end{aligned} \quad (\text{A13})$$

The final step consists in inserting the above result (A12) into the expression (A1) of the correlation function. This leads to Eqs. (3)-(6). The calculation of the two-point correlation function then reduces to a double series of terms that are given by the integral of a Gaussian function over a rectangular domain, the size of which is given by ℓ . This series has been computed numerically in order to obtain the figures of the paper.

Let us now treat the case where $\det M = 0$. We first consider the situation where $t_b \rightarrow t_a$ (meaning $r_b \rightarrow r_a$ and $\varphi_b \rightarrow \varphi_a$). In this limit, one can write

$$\lim_{t_b \rightarrow t_a} \langle \tilde{Q} | \hat{U}_a \hat{U}_b^\dagger | \bar{Q} \rangle = \frac{1}{\sqrt{\pi}} \frac{1}{\cosh r_a \sqrt{\det M}/8} \exp \left[-\frac{(\bar{Q} - \tilde{Q})^2}{(\cosh r_a \sqrt{\det M}/8)^2} \right]. \quad (\text{A14})$$

Then, if we define a small parameter by $\epsilon \equiv \cosh r_a \sqrt{\det M}/8$ which, obviously, goes to zero since $\det M \rightarrow 0$, then Eq. (A14) reduces to

$$\lim_{t_b \rightarrow t_a} \langle \tilde{Q} | \hat{U}_a \hat{U}_b^\dagger | \bar{Q} \rangle = \lim_{\epsilon \rightarrow 0} \frac{1}{\epsilon \sqrt{\pi}} e^{-(\bar{Q} - \tilde{Q})^2 / \epsilon^2} = \delta(\bar{Q} - \tilde{Q}). \quad (\text{A15})$$

As a consequence, in this limit, the correlation function (A1) takes the form

$$\lim_{t_b \rightarrow t_a} C_{ab} = \sum_{n=-\infty}^{n=+\infty} \sum_{m=-\infty}^{m=+\infty} (-1)^{n+m} \int_{n\ell}^{(n+1)\ell} \int_{m\ell}^{(m+1)\ell} d\tilde{Q} d\bar{Q} \Re \left[\Psi_{1\text{sq}}^*(t_a, \tilde{Q}) \Psi_{1\text{sq}}(t_a, \bar{Q}) \delta(\bar{Q} - \tilde{Q}) \right] \quad (\text{A16})$$

$$= \sum_{n=-\infty}^{n=+\infty} \int_{n\ell}^{(n+1)\ell} d\tilde{Q} \Psi_{1\text{sq}}^*(t_a, \tilde{Q}) \Psi_{1\text{sq}}(t_a, \tilde{Q}) = 1, \quad (\text{A17})$$

and one verifies that the correlation function is indeed one when the two times t_a and t_b coincide.

Let us finally focus on the case where $\varphi_a = \varphi_b = \varphi \rightarrow 0$ but $r_a \neq r_b$. In this situation, one can define a new small parameter ϵ by $\epsilon^2 \equiv -2i\varphi(e^{2r_a} - e^{2r_b})$ and one has

$$\lim_{\varphi_b \rightarrow \varphi_a} \langle \tilde{Q} | \hat{U}(t_a) \hat{U}^\dagger(t_b) | \bar{Q} \rangle = e^{(r_a + r_b)/2} \lim_{\epsilon \rightarrow 0} \frac{1}{\epsilon \sqrt{\pi}} e^{-(e^{r_b} \bar{Q} - e^{r_a} \tilde{Q})^2 / \epsilon^2} = e^{(r_a + r_b)/2} \delta(e^{r_b} \bar{Q} - e^{r_a} \tilde{Q}). \quad (\text{A18})$$

As a consequence, the two-point correlation function (A1) can now be re-expressed as

$$\lim_{\varphi_b \rightarrow \varphi_a} C_{ab} = e^{(r_a + r_b)/2} \sum_{n=-\infty}^{n=+\infty} \sum_{m=-\infty}^{m=+\infty} (-1)^{n+m} \int_{n\ell}^{(n+1)\ell} \int_{m\ell}^{(m+1)\ell} d\tilde{Q} d\bar{Q} \Re \left[\Psi_{1\text{sq}}^*(t_a, \tilde{Q}) \Psi_{1\text{sq}}(t_b, \bar{Q}) \delta(e^{r_b} \bar{Q} - e^{r_a} \tilde{Q}) \right]. \quad (\text{A19})$$

A first integration can be performed thanks to the presence of the Dirac function. Then the remaining one can also be performed and the result can be expressed in terms of error functions. This leads to the formulas given in the main text. It is interesting to note that the case where the squeezing angles vanish can only be defined through the limiting procedure explained above since, taken at face value, the integral in Eq. (A4) is divergent in this situation.

Finally, let us note that simple expressions can be derived in the limit $\ell \rightarrow \infty$. In this case, the spin operator \hat{S}_z defined in Eq. (1) is simply the sign operator, i.e. it returns 1 if $Q \geq 0$ and -1 if $Q < 0$. In this limit, the double sum of Eq. (A1) only contains four terms, corresponding to $(n, m) = (0, 0), (-1, 0), (0, -1), (-1, -1)$, which are Gaussian integrals and can therefore be calculated. One obtains

$$C_{ab}(\ell \rightarrow \infty) = \Re \left\{ -\frac{4A(a, b)}{\sqrt{B^2(a, b) - 4A(a, b)A^*(b, a)}} \operatorname{arctanh} \left[\frac{B(a, b)}{\sqrt{B^2(a, b) - 4A(a, b)A^*(b, a)}} \right] \right\}. \quad (\text{A20})$$

-
- [1] A. Einstein, B. Podolsky, and N. Rosen, Phys. Rev. **47**, 777 (1935).
 - [2] J. S. Bell, Physics **1**, 195 (1964).
 - [3] J. F. Clauser, M. A. Horne, A. Shimony, and R. A. Holt, Phys. Rev. Lett. **23**, 880 (1969).
 - [4] A. Aspect, J. Dalibard, and G. Roger, Phys. Rev. Lett. **49**, 1804 (1982).
 - [5] A. Aspect, P. Grangier, and G. Roger, Phys. Rev. Lett. **49**, 91 (1982).
 - [6] A. J. Leggett and A. Garg, Phys. Rev. Lett. **54**, 857 (1985).
 - [7] C. Emary, N. Lambert, and F. Nori, Reports on Progress in Physics **77**, 016001 (2014), 1304.5133.
 - [8] A. Palacios-Laloy, F. Mallet, F. Nguyen, P. Bertet, D. Vion, D. Esteve, and A. N. Korotkov, Nature Physics **6**, 442 (2010), 1005.3435.
 - [9] J. Koch, T. M. Yu, J. Gambetta, A. A. Houck, D. I. Schuster, J. Majer, A. Blais, M. H. Devoret, S. M. Girvin, and R. J. Schoelkopf, Phys. Rev. A **76**, 042319 (2007).
 - [10] J. P. Groen, D. Ristè, L. Tornberg, J. Cramer, P. C. de Groot, T. Picot, G. Johansson, and L. DiCarlo, Physical Review Letters **111**, 090506 (2013), 1302.5147.
 - [11] G. C. Knee, K. Kakuyanagi, M.-C. Yeh, Y. Matsuzaki, H. Toida, H. Yamaguchi, S. Saito, A. J. Leggett, and W. J. Munro, Nature Communications **7**, 13253 (2016), 1601.03728.
 - [12] R. Ruskov, A. N. Korotkov, and A. Mizel, Physical Review Letters **96**, 200404 (2006), quant-ph/0505094.
 - [13] C. M. Caves and B. L. Schumaker, Phys. Rev. **A31**, 3068 (1985).
 - [14] B. L. Schumaker and C. M. Caves, Phys. Rev. **A31**, 3093 (1985).

- [15] L.-A. Wu, H. J. Kimble, J. L. Hall, and H. Wu, *Phys. Rev. Lett.* **57**, 2520 (1986).
- [16] T. Eberle, S. Steinlechner, J. Bauchrowitz, V. Handchen, H. Vahlbruch, M. Mehmet, H. Muller-Ebhardt, and R. Schnabel, *Phys. Rev. Lett.* **104**, 251102 (2010), 1007.0574.
- [17] O. V. Misochko, J. Hu, and K. G. Nakamura, *Physics Letters A* **375**, 4141 (2011), 1011.2001.
- [18] J. S. Schwinger, *Phys. Rev.* **82**, 664 (1951).
- [19] W. G. Unruh, *Phys. Rev.* **D14**, 870 (1976).
- [20] S. W. Hawking, *Commun. Math. Phys.* **43**, 199 (1975).
- [21] A. A. Starobinsky, *Phys. Lett.* **B91**, 99 (1980).
- [22] A. H. Guth, *Phys. Rev.* **D23**, 347 (1981).
- [23] A. D. Linde, *Phys. Lett.* **B108**, 389 (1982).
- [24] P. A. R. Ade et al. (Planck), *Astron. Astrophys.* **594**, A13 (2016), 1502.01589.
- [25] P. A. R. Ade et al. (Planck), *Astron. Astrophys.* **594**, A20 (2016), 1502.02114.
- [26] J. Martin, C. Ringeval, and V. Vennin, *Phys. Dark Univ.* **5-6**, 75–235 (2014), 1303.3787.
- [27] J. Martin, C. Ringeval, R. Trotta, and V. Vennin, *JCAP* **1403**, 039 (2014), 1312.3529.
- [28] J. Martin, C. Ringeval, and V. Vennin, *Phys. Rev. Lett.* **114**, 081303 (2015), 1410.7958.
- [29] J. Martin, *Astrophys. Space Sci. Proc.* **45**, 41 (2016), 1502.05733.
- [30] L. Grishchuk and Y. Sidorov, *Phys. Rev.* **D42**, 3413 (1990).
- [31] J. Martin, *Lect. Notes Phys.* **738**, 193 (2008), 0704.3540.
- [32] J. Martin, V. Vennin, and P. Peter, *Phys. Rev.* **D86**, 103524 (2012), 1207.2086.
- [33] J. Martin and V. Vennin, *Phys. Rev.* **D93**, 023505 (2016), 1510.04038.
- [34] J. Aasi et al. (LIGO Scientific), *Nature Photon.* **7**, 613 (2013), 1310.0383.
- [35] I. D. Leroux, M. H. Schleier-Smith, and V. Vuletić, *Phys. Rev. Lett.* **104**, 250801 (2010).
- [36] S. L. Braunstein and P. van Loock, *Rev. Mod. Phys.* **77**, 513 (2005).
- [37] C. Budroni, G. Vitagliano, G. Colangelo, R. J. Sewell, O. Gühne, G. Tóth, and M. W. Mitchell, *Physical Review Letters* **115**, 200403 (2015), 1503.08433.
- [38] N. Lambert, K. Debnath, A. F. Kockum, G. C. Knee, W. J. Munro, and F. Nori, *Phys. Rev. A* **94**, 012105 (2016), 1604.04059.
- [39] J.-Å. Larsson, *Phys. Rev. A* **70**, 022102 (2004), quant-ph/0310140.
- [40] K. Banaszek and K. Wódkiewicz, *Phys. Rev. Lett.* **82**, 2009 (1999).
- [41] Z.-B. Chen, J.-W. Pan, G. Hou, and Y.-D. Zhang, *Phys. Rev. Lett.* **88**, 040406 (2002).
- [42] J. Martin and V. Vennin, *Phys. Rev.* **A93**, 062117 (2016), 1605.02944.
- [43] W. H. Zurek, *Phys. Rev.* **D24**, 1516 (1981).
- [44] W. H. Zurek, *Phys. Rev.* **D26**, 1862 (1982).
- [45] E. Joos and H. D. Zeh, *Z. Phys.* **B59**, 223 (1985).
- [46] J.-S. Xu, C.-F. Li, X.-B. Zou, and G.-C. Guo, *Scientific Reports* **1**, 101 (2011).
- [47] C. King and M. B. Ruskai, *IEEE Transactions on Information Theory* **47** (2001), quant-ph/9911079.
- [48] C. Emary, *Phys. Rev. A* **87**, 032106 (2013), 1212.3865.
- [49] A. E. Rastegin, *Annals of Physics* **355**, 241 (2015), 1410.7889.
- [50] K. Ando and V. Vennin, *Phys. Rev. A* **102**, 052213 (2020), 2007.00458.